

Preparation and Catalytic Performance of Fe₃O₄ Based Nanocomposite

Muhammad Irfan^{1*}, Amir Zeeshan², Muhammad Daniyal Nadeem³, Maryam Liaquat⁴, Mirza Haider Ali⁵, Muhammad Iqbal Tabassum⁶, Shizza Rehman⁷

¹Government College University Faisalabad, Pakistan

²Government College University Faisalabad, Pakistan

³Government College University Lahore, Pakistan

⁴College of Electronics and Information Engineering, Shenzhen university, Shenzhen 518060, China

⁵Lahore Garrison university Lahore, Pakistan

⁶University of Engineering and Technology Lahore, Pakistan

⁷Khawaja Fareed university of Engineering and Information Technology, Pakistan

DOI: <https://doi.org/10.36347/sjet.2025.v13i02.005>

| Received: 06.01.2025 | Accepted: 13.02.2025 | Published: 17.02.2025

*Corresponding author: Muhammad Irfan
Government College University Faisalabad, Pakistan

Abstract

Original Research Article

Fe₃O₄-based nanocomposites were synthesized using iron salts, glucose, and ammonium hydroxide for catalytic adsorption of methyl orange and malachite green dyes from wastewater. The nanocomposites were characterized using UV-VIS Spectroscopy, SEM, XRD, and FTIR to analyze their surface morphology, crystallinity, and functional groups. Results showed high adsorption efficiency, with 83.9% removal of methyl orange and 61-75% removal of malachite green. The exceptional properties of Fe₃O₄ nanocomposites, including superparamagnetic, large surface area, and low toxicity, contribute to their effectiveness in dye removal. Multi-cycle usability and regeneration with ethanol or acetone improved adsorption performance, making them a cost-effective and sustainable solution. The dye-loaded composites were properly washed with distilled water and reused, maintaining adsorption efficiency. Their excellent recyclability and adsorption capabilities make Fe₃O₄ nanocomposites a viable option for scalable wastewater treatment applications, offering an efficient and environmentally friendly approach for dye removal.

Keywords: Fe₃O₄ nanocomposites, catalytic adsorption, wastewater treatment, methyl orange, malachite green, regeneration, recyclability, superparamagnetic.

Copyright © 2025 The Author(s): This is an open-access article distributed under the terms of the Creative Commons Attribution 4.0 International License (CC BY-NC 4.0) which permits unrestricted use, distribution, and reproduction in any medium for non-commercial use provided the original author and source are credited.

1. INTRODUCTION

Nanoscience is the study of materials and systems at the nanoscale (1-100 nm), where properties and behaviors differ significantly from their bulk counterparts (Chen *et al.*, 2009). As a multidisciplinary field encompassing physics, chemistry, engineering, biology, and medicine, nanoscience has led to advancements in biotechnology, particularly in drug delivery and vaccine development. For example, the ability of synthetic and natural nanomaterials to mimic the structure of viruses has contributed to the creation of novel vaccine platforms, including those targeting SARS-CoV-2 (Algar *et al.*, 2022). Nanotechnology, a key branch of nanoscience, has revolutionized various industries, including medicine, cosmetics, and environmental remediation. The application of nanoparticles (NPs) in cosmetics, for instance, has enhanced product performance by improving absorption and stability (Mihriyan *et al.*, 2012). However, concerns about potential long-term toxicity and public

skepticism have led to regulatory changes, such as the European Union's restrictions on nanoparticle use in cosmetics (Brazell, 2012). In medicine, nanotechnology has significantly improved disease diagnosis and treatment, with FDA-approved nanomaterials now used in chemotherapy, imaging, and targeted drug delivery (Kirtane *et al.*, 2021).

Nanoparticles, characterized by at least one dimension in the 1-100 nm range, exhibit unique physicochemical properties, including a high surface-to-volume ratio and increased reactivity (Garcia *et al.*, 2018). Magnetite nanoparticles (Fe₃O₄), in particular, are known for their superparamagnetic properties, biocompatibility, and environmental stability. These features make them suitable for applications in targeted drug delivery, imaging, and catalysis (Mahmoodabadi *et al.*, 2018). Their ability to enhance mechanical, thermal, and electrical properties when incorporated into composites has also led to their widespread use in

material science and engineering (Chen *et al.*, 2021). Despite their numerous advantages, nanoparticles also present potential health risks. Factors such as particle size, shape, and surface chemistry influence their toxicity. Low-solubility nanoparticles have been linked to cancer due to their increased chemical and biological reactivity (Parhi, 2022). Exposure through inhalation, ingestion, or skin contact may lead to bioaccumulation and adverse health effects. For instance, studies have shown that cobalt and chromium nanoparticles can penetrate the skin barrier and cause cellular damage (Sinitsyna & Vetcher, 2022).

Nanocomposites, which integrate nanoparticles with other materials like polymers, ceramics, or metals, have emerged as a promising class of materials with superior mechanical, thermal, and chemical properties. Magnetic iron oxide nanocomposites, such as Fe₃O₄-based systems, have gained attention due to their high magnetic saturation, stability, and biocompatibility (Novoselova, 2021). These materials are widely used in drug delivery, wastewater treatment, and catalysis. Iron oxide nanocomposites are particularly effective in environmental applications, where they serve as

adsorbents for pollutants and catalysts for degradation reactions (Eskandarinezhad *et al.*, 2021). The synthesis of Fe₃O₄-based nanocomposites involves various methods, including co-precipitation, thermal decomposition, and sol-gel techniques (Kumar & Gangawane, 2022). Each method offers different advantages in terms of particle size control, surface modification, and scalability. The properties of these nanocomposites, such as stability, surface area, and functionalization, play a crucial role in determining their efficiency in specific applications (Wang *et al.*, 2022).

This study aims to synthesize Fe₃O₄-based nanocomposites and evaluate their catalytic adsorption properties for removing dyes from wastewater. The research is divided into three objectives: (i) synthesis of Fe₃O₄ nanocomposites using the co-precipitation method, (ii) characterization of the synthesized materials using SEM, XRD, and FT-IR spectroscopy, and (iii) analysis of their catalytic adsorption efficiency in dye removal (Taha *et al.*, 2022). The findings will contribute to the development of cost-effective and environmentally friendly solutions for water purification.

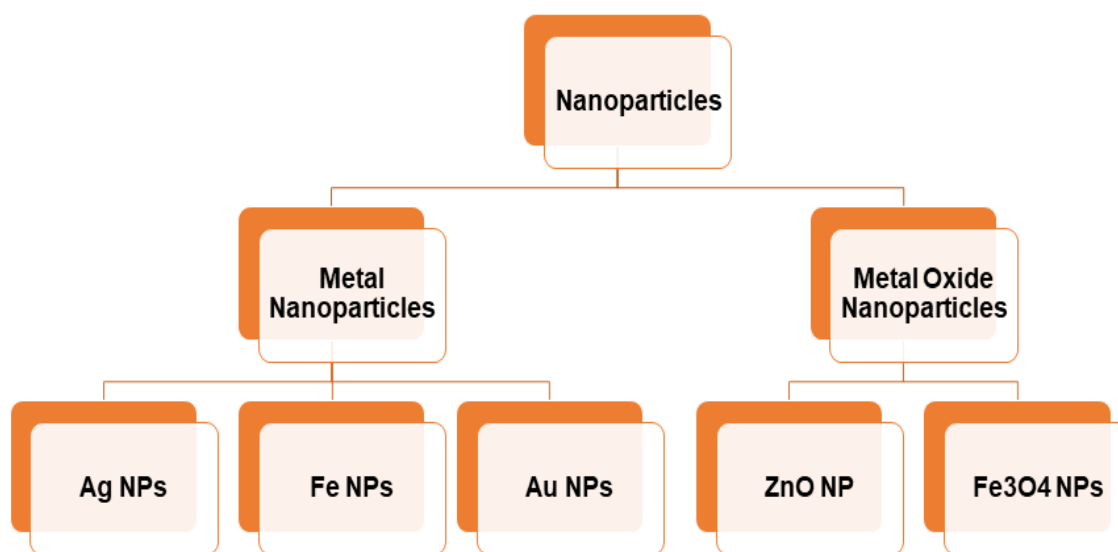


Figure 1.1: Flow chart of the nanoparticles and their classes

2. LITERATURE REVIEW

Fe₃O₄-based magnetic nanoparticles have become widely recognized for their diverse industrial applications, including in biomedical fields, wastewater treatment, carbon capture, data storage, and magnetic inks (Dudchenko *et al.*, 2022). These nanoparticles offer unique advantages, such as superparamagnetism, high surface area, and biocompatibility, which are essential for drug delivery, environmental remediation, and catalytic processes (Koo *et al.*, 2019). Various synthesis methods have been developed to produce Fe₃O₄ nanoparticles with controlled size and shape, such as room temperature co-precipitation (Norfolk, 2021), microwave-assisted synthesis (Elazab Dr, 2019), and

solvothermal techniques (Zhu *et al.*, 2021). Additionally, Fe₃O₄ nanoparticles have been used in diverse catalytic applications, such as the reduction of 4-nitrophenol (Thu *et al.*, 2017), dye removal (Yilmaz *et al.*, 2022), and as catalysts for indole derivative synthesis (Rostami *et al.*, 2018). Advances in functionalization, such as modifying Fe₃O₄ with chitosan (Cuana *et al.*, 2022) and silver nanoparticles (Chen *et al.*, 2021), have enhanced their catalytic and antibacterial properties. Moreover, these nanoparticles have shown significant promise in cancer therapy by inducing apoptosis in cancer cells (Namvar *et al.*, 2014). Furthermore, their incorporation into composite materials has improved their performance in various applications, from photocatalysis (Shekofteh-

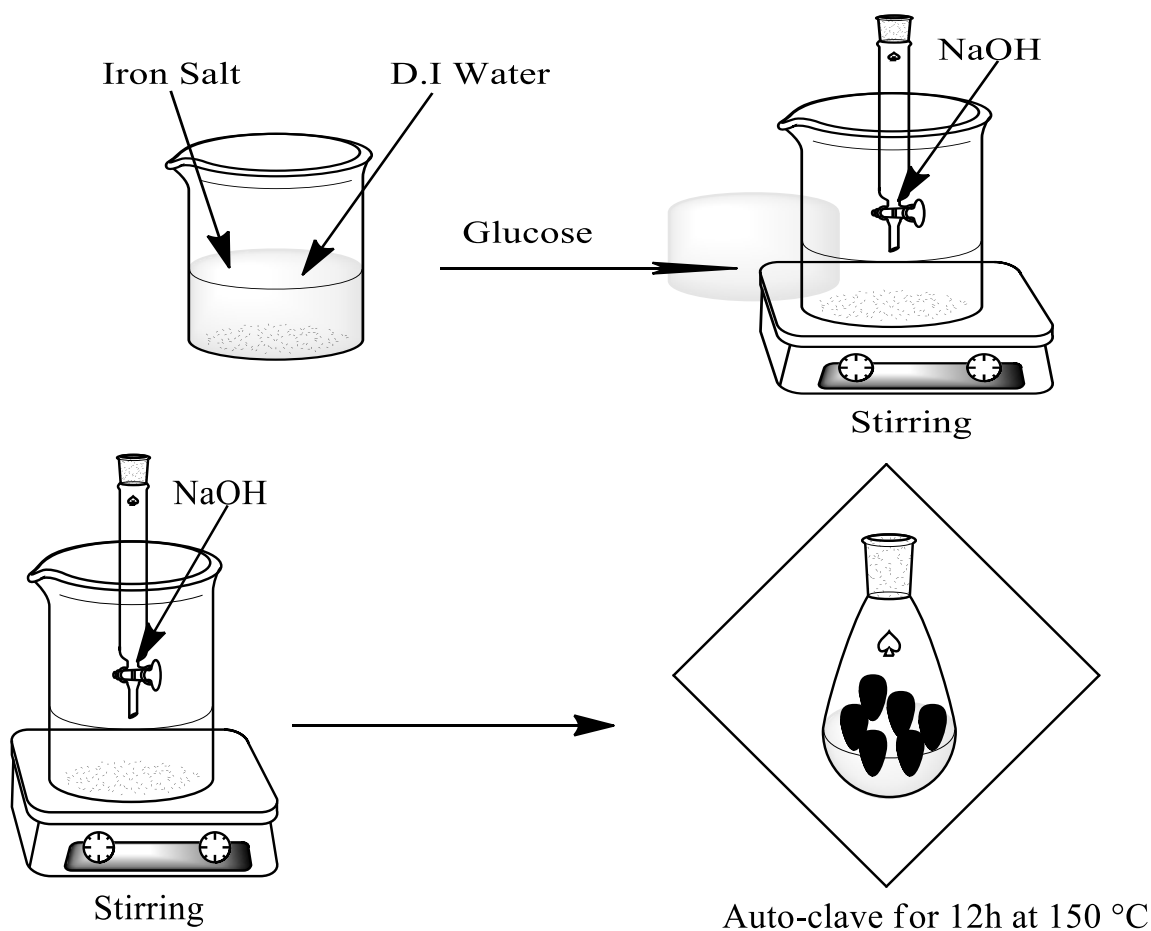
Gohari & Habibi-Yangjeh, 2016) to enhancing electromagnetic interference shielding (Cai *et al.*, 2022). These studies demonstrate the versatility and potential of Fe_3O_4 -based magnetic nanocomposites in a broad range of scientific and industrial fields.

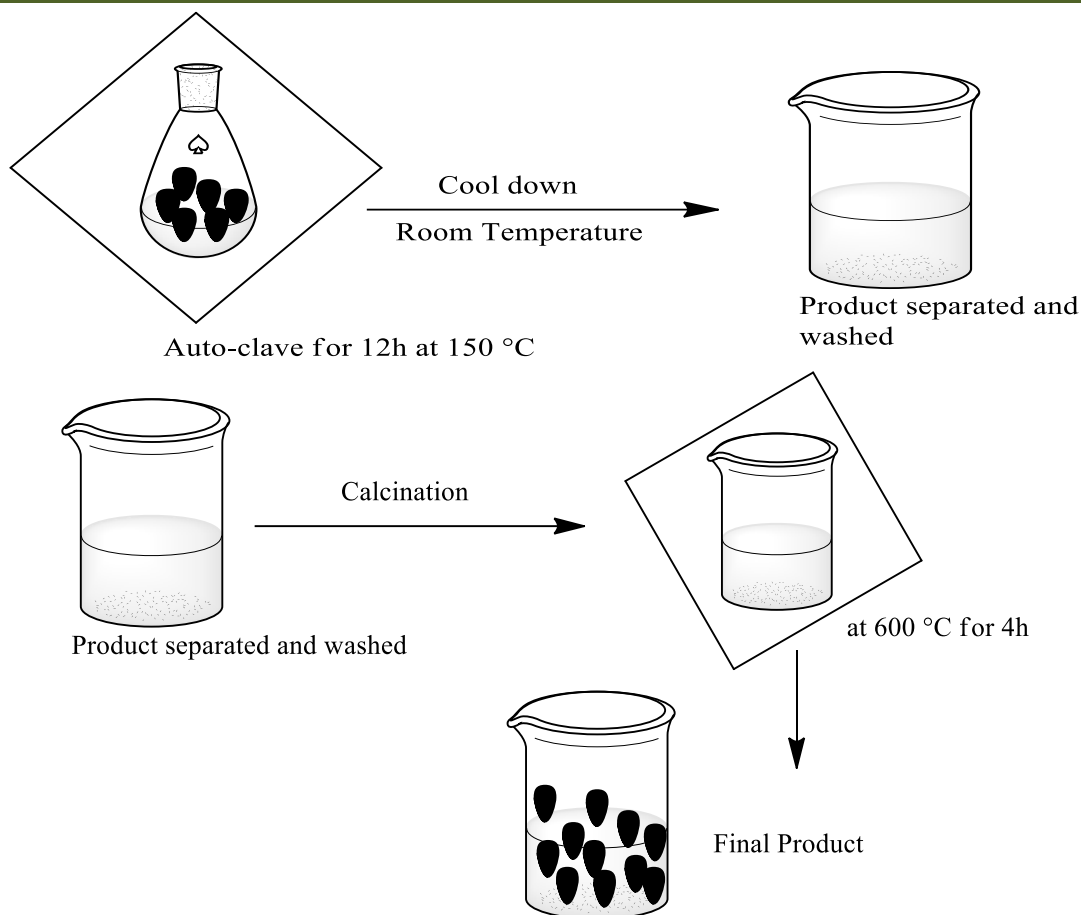
3. RESEARCH METHODOLOGY

The research employed analytical-grade chemicals sourced from Merck UK, including ferric chloride, ferrous chloride, NH_4OH (30% ammonia), sodium hydroxide (1N), ethanol, glucose, malachite green dye, and methyl orange dye, which were obtained from Lahore Garrison University. Standard laboratory glassware such as beakers, pipettes, burettes, conical flasks, test tubes, thermometers, measuring cylinders, and filter paper were used. Equipment included a magnetic hotplate, stands, and a furnace. Analytical instruments included a Chiyo Japan bench-top balance with 0.1g accuracy, an oven for heating, a muffle furnace for high-temperature treatments, a powder X-ray diffractometer for crystal structure analysis, an FT-IR spectrophotometer for functional group identification, a UV-VIS spectrophotometer for composite analysis, and a scanning electron microscope (FEI Nova Nano SEM) for surface morphology and composition

characterization. Stock solutions of 1000 ppm methyl orange and malachite green dyes were prepared for catalytic adsorption by Fe_3O_4 nanocomposite. All chemicals for synthesis were obtained from the chemistry department.

The co-precipitation method was employed as it is a simple, safe, and cost-effective technique for synthesizing nanocomposites. This method requires lower synthesis temperatures compared to other conventional techniques, making it advantageous for large-scale production. Iron salts were mixed with glucose in de-ionized water. The solution was stirred on a magnetic hotplate, and a base was added to enhance the reaction rate. The reaction mixture was transferred into a 100 ml Teflon flask and placed in an autoclave at 150°C for 12 hours. After heating, the solution was allowed to cool to room temperature. The product was separated using an external magnetic field, washed several times with de-ionized water and alcohol, and then dried in an oven for 12 hours (Xu *et al.*, 2014). The final product was calcined in a muffle furnace at 600°C for 4 hours and then collected for further processing. Once prepared, the sample was characterized using SEM, XRD, and FT-IR spectroscopy to analyze its morphology, crystallinity, and functional groups (Rasoulzadeh *et al.*, 2019).





4. RESULT AND DISCUSSION

The magnetite (Fe_3O_4) nanocomposite has been prepared through Co-precipitation method. To explore the size, shape, composition, and functional group of nano-composite, several characterization approaches have been developed. The basic strategies for characterizing these critical characteristics are discussed below.

4.1 Scanning Electron Microscopy

SEM was used to examine the surface morphology and chemical composition of the Fe_3O_4 nanocomposite. The images confirmed the synthesis of Fe_3O_4 -based nanocomposite, showing its structure and a carbon shell that increases the surface area, consistent with literature data. The morphology was analyzed using a TLD detector at micro- and nano-scale levels. High-resolution SEM typically requires conductive substrates, but nonconductive materials can be imaged using environmental SEM at low pressure or by coating them with a thin (5–10 nm) metallic layer for improved resolution.

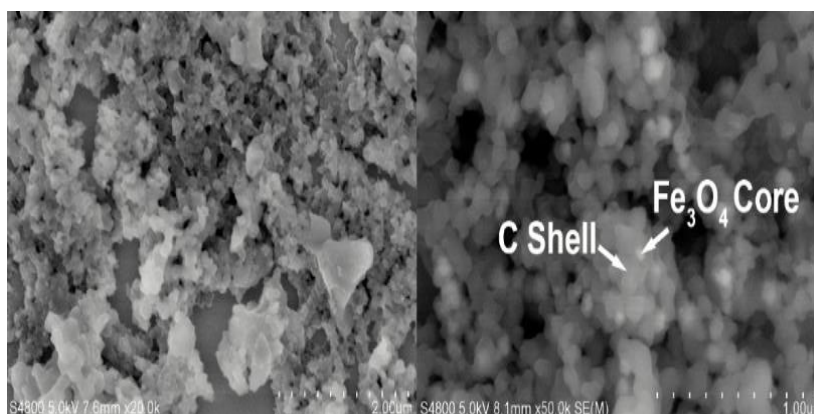


Fig. 4.1: SEM image of Fe_3O_4 based nanocomposite

4.2 X-Ray Diffraction

XRD analysis confirmed the crystalline structure of Fe_3O_4 nanocomposite, with peaks at 33.312° , 35.426° , 49.641° , and 54.286° , indicating partial

crystallinity. The diffraction pattern revealed both crystalline and amorphous phases. Changes in calcination temperature influenced particle size, confirming structural modifications during synthesis.

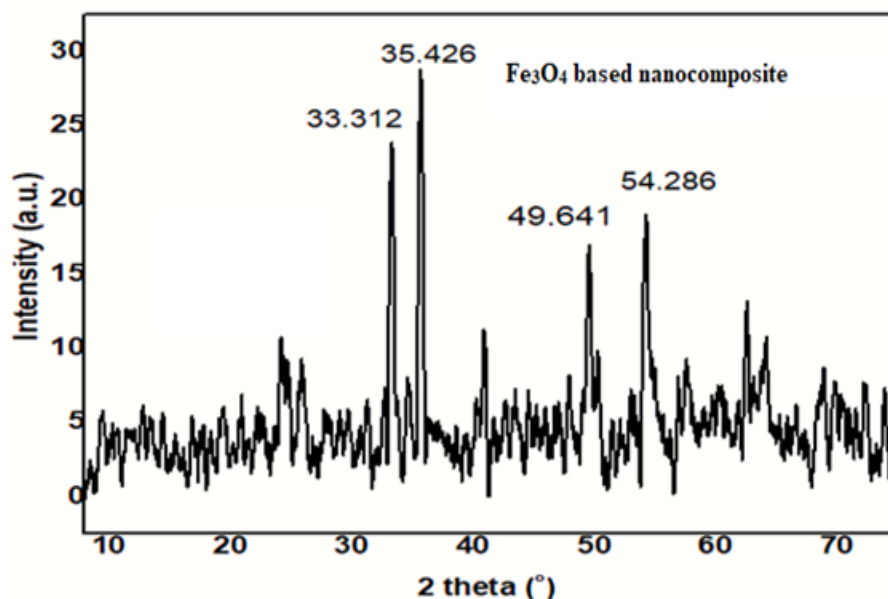


Fig. 4.2: XRD analysis of Fe_3O_4 based nanocomposite

4.3 Fourier Transform Infrared Spectroscopy (FT-IR)

The Fourier Transform Infrared Spectroscopy (FT-IR) analysis was conducted to identify functional groups present in Fe_3O_4 -based nanocomposites. The FT-IR spectra confirmed the presence of specific functional groups such as phenols, amides, and aromatic compounds, which have a high binding affinity for iron (Fe). Key peaks around 410 cm^{-1} and 650 cm^{-1} were associated with Fe-O bonds, while additional peaks at 352 cm^{-1} , 400 cm^{-1} , 470 cm^{-1} , 540 cm^{-1} , and 570 cm^{-1} indicated different iron oxide phases, including

magnetite and maghemite. The Fe-O stretching vibration was observed at 622.58 cm^{-1} . A broad band at 3265 cm^{-1} was linked to O-H stretching vibrations, indicating the presence of water or hydroxyl groups on the magnetite surface. Other absorption bands included 1396 cm^{-1} (phenolic O-H bending), 1627 cm^{-1} (C=O stretching in carbonyl groups), and 1034 cm^{-1} (C-O stretching of alcohol groups). The results confirmed the strong crystallinity of Fe_3O_4 nanocomposites, with characteristic Fe-O vibrations detected in the $400\text{-}600\text{ cm}^{-1}$ range.

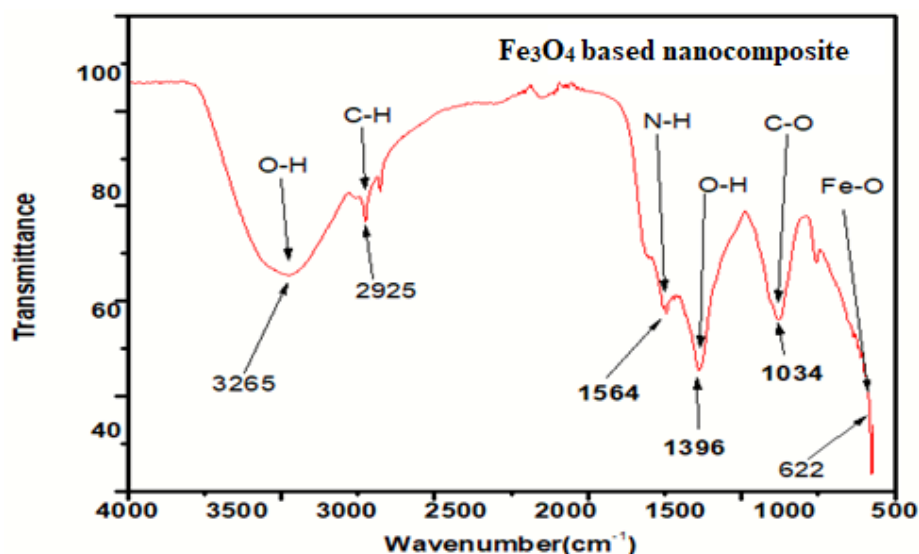


Fig. 4.3: FT-IR analysis of Fe_3O_4 based nanocomposite

4.4 Catalytic Adsorption of dyes by Fe₃O₄ based Nanocomposites

4.4.1 Adsorption Experiments

Batch adsorption experiments were conducted to evaluate the adsorption efficiency of Fe₃O₄ nanocomposites for methyl orange (MO) and malachite green (MG) dyes. A solution containing 2.5 mg of adsorbent and 10 mL of dye solution (1000 ppm) was prepared in a 150 mL conical flask. The concentration of dyes was measured using a Shimadzu UV-Vis spectrophotometer at 464 nm for MO and 624 nm for MG. The adsorption efficiency and capacity were determined using the Beer-Lambert law, providing insights into the removal performance of the nanocomposites. The dye removal efficiency (θ) and adsorption capacity (q_e , mg g⁻¹) can be calculated from following equation:

$$\text{Removal Efficiency}(\theta) = \frac{C_0 - C_e}{C_0} * 100 \dots\dots\dots 1$$

$$\text{Adsorption Capacity}(q_e) = \frac{(C_0 - C_e)V}{m} \dots\dots\dots 2$$

where C₀ and C_e are the initial and equilibrium concentration (mgL⁻¹) of dye, respectively; V and m are the volume of solution (L) and mass of the adsorbent (g), respectively.

4.4.2 Adsorption Kinetics

The adsorption rate curves of MO and MG are presented below, and the adsorption speed of both MO

and MG on the adsorbents is very fast, with adsorption equilibrium reached in less than 20 minutes. The linear pseudo-first-order and pseudo-second-order kinetic equations are utilized to better understand the properties of the adsorption process.

$$\log(q_e - qt) = \log q_e - \frac{k_1}{2.303} t \dots\dots\dots 4$$

$$\frac{t}{qt} = \frac{1}{k_2 q_e^2} + \frac{t}{q_e} \dots\dots\dots 5$$

In all cases, the pseudo-second-order kinetic model fit better than the pseudo-first-order kinetic model, with higher correlation coefficient values and calculated adsorption capacities ($q_{e,cal}$) that were closer to experimental data ($q_{e,exp}$), indicating that this model is better suited to describe MO and MG adsorption on the studied samples.

4.4.3 Methyl Orange (MO) Dye.

The methyl orange (MO) dye has a molecular weight of 327.34g/mol and a chemical formula of C₁₄H₁₄N₃NaO₃S, respectively. Using distilled water, a stock solution of the investigated dye containing 1000 mg/L was made. To achieve the required dye concentration, a working solution diluted from a stock solution was used in the current study (Yadav & Dasgupta, 2022).

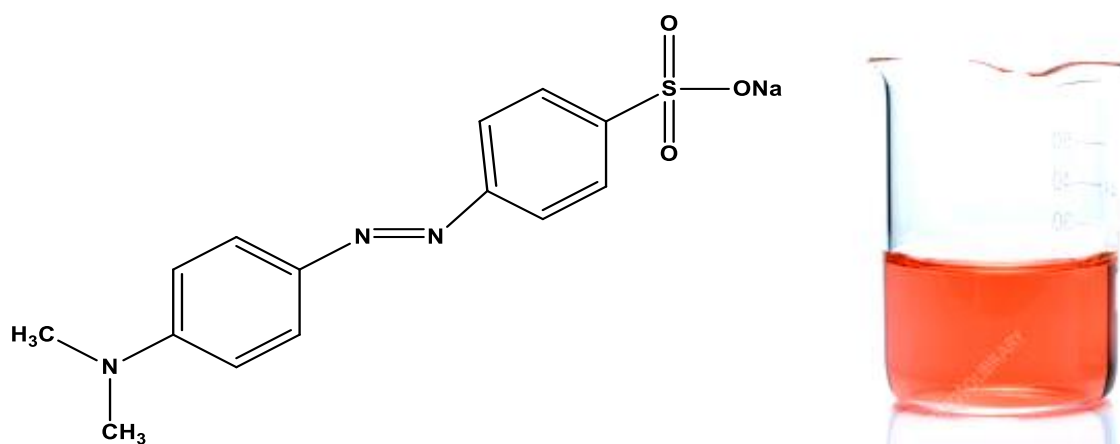


Fig. 4.4: Methyl orange structural formula and Solution of Methyl orange

4.4.3.1 Effect of Contact Time.

Figure demonstrates how the amount of MO dye removed depends on the period of contact time. The adsorption efficiency of methyl orange (MO) increased with time, reaching a maximum removal of 83.9% within

20 minutes using Fe₃O₄ nanocomposites. Initially, the adsorption rate was high due to the availability of active sites, but as these sites became occupied, the process slowed down and reached equilibrium (Sarojini *et al.*, 2023).

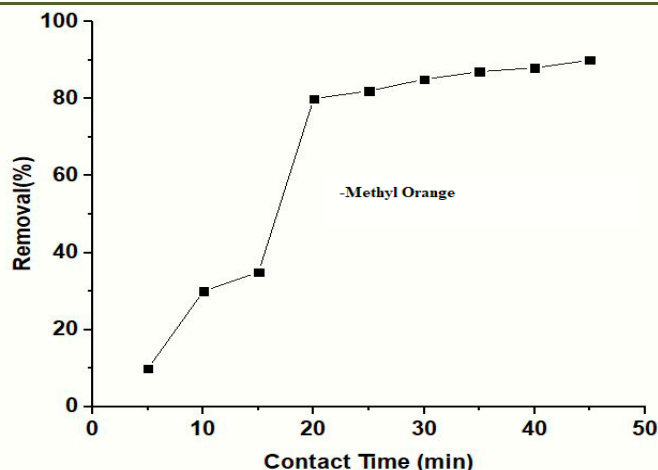


Fig. 4.5: Effect of contact time on removal of methyl orange

4.4.3.2 Effect of Catalyst Dose.

The amount of catalyst used significantly influenced MO removal. Increasing the catalyst dosage from 0.5 to 2.5 mg/10ml enhanced adsorption, with the

highest efficiency observed at 2 mg/10ml. Beyond this point, no significant improvement was noted, indicating that all active sites were occupied, limiting further adsorption (Bassyouni *et al.*, 2019).

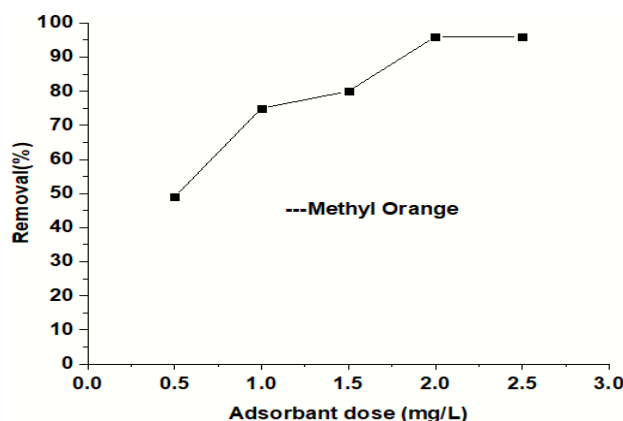


Fig. 4.6: Effect of adsorbent dosage on removal of methyl orange

4.4.3.3 Effect of pH on the removal of M.O.

The pH level of the dye solution affected adsorption efficiency, with pH 5.0 being the optimal condition. At this pH, the adsorbent had a positive surface charge, enhancing electrostatic attraction with

the negatively charged MO dye. In contrast, at higher pH levels, the adsorbent's surface became negatively charged, leading to repulsion and lower adsorption efficiency. Therefore, pH 5.0 was used in the research that followed (Wang & Yan, 2021).

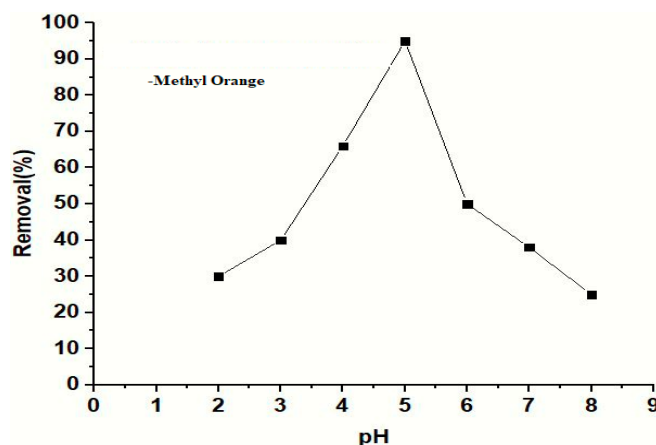


Figure 4.7: Effect of pH on removal of methyl orange

4.4.3.4 Effect of dye concentration on the MO removal rate.

Batch experiments conducted with MO concentrations ranging from 20 to 200 mg/L revealed that higher concentrations reduced adsorption efficiency.

This was due to the rapid saturation of available adsorption sites. Under optimal conditions, an equilibrium capacity of 80 mg/L was maintained, where adsorption efficiency was maximized (Mishra *et al.*, 2019).

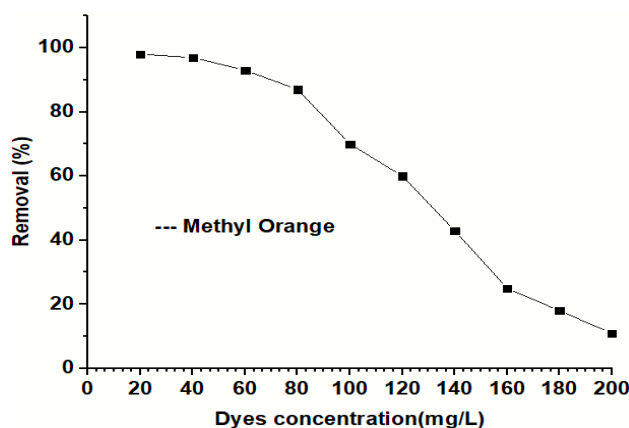


Fig. 4.8: Effect of dye concentration on removal of methyl orange

4.4.3.5 Effect of temperature on the MO removal rate.

Temperature played a significant role in MO removal, with adsorption rates increasing as the reaction temperature rose from 20°C to 50°C. Higher

temperatures enhanced the diffusion of dye molecules into the Fe₃O₄ nanocomposite. The optimal temperature was determined to be 40°C, balancing adsorption efficiency and cost-effectiveness.

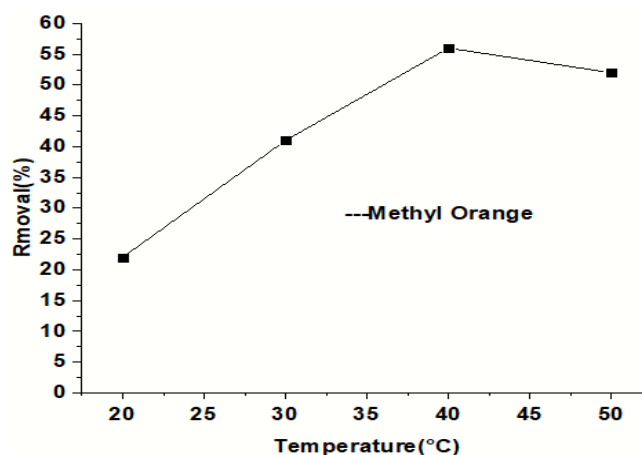


Fig. 4.9: Effect of temperature on removal of methyl orange

4.4.4 Malachite Green (M.G) Dye

Malachite Green (MG) dye having molecular weight of 364.91g/mol and a chemical formula of C₂₃H₂₅ClN₂, respectively (Figure). Using distilled water,

a stock solution of the identify dyes containing 1000 mg/L was made. To achieve the required dye concentration, a working solution diluted from a stock solution was used in the current study.

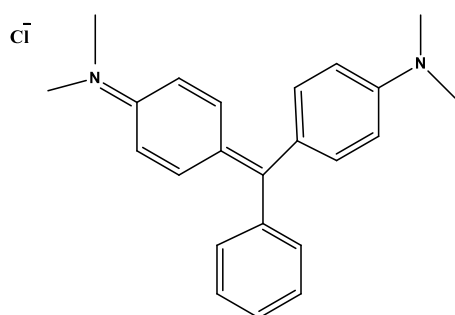


Fig. 4.10: Malachite Green structural formula and Solution of Malachite Green dye

4.4.4.1 Effect of pH on removal rate.

The adsorption efficiency of MG dye varied with pH. The removal rate increased from 51% at pH 3 to 86% at pH 9, indicating that higher pH levels enhanced

adsorption. This was due to the negatively charged catalyst surface at higher pH, which strengthened the attraction to the cationic MG dye (Magdalane *et al.*, 2017).

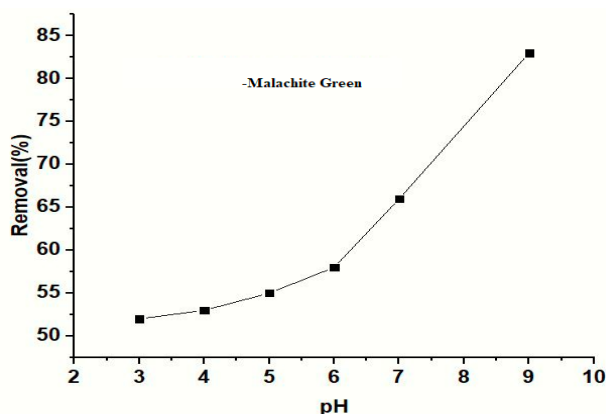


Fig. 4.11: Effect of pH on the removal of malachite green

4.4.4.2 Effect of contact time.

The removal efficiency of MG improved with increasing contact time. Within 20 minutes, 20% of the dye was removed, which rose to 60% at 30 minutes and

peaked at 75% after 40 minutes. This trend demonstrated that adsorption was initially rapid due to the availability of active sites before reaching equilibrium (Amoli-Diva *et al.*, 2019).

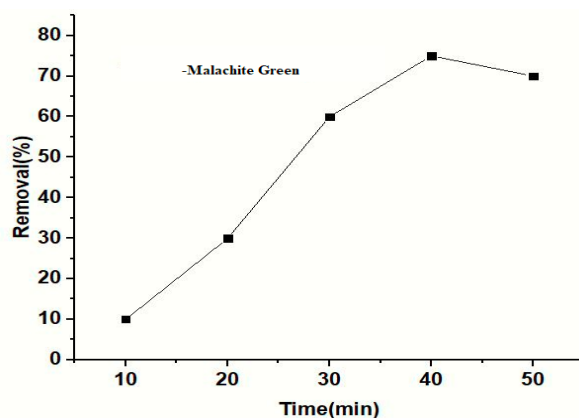


Fig. 4.12: Effect of contact time on the removal of malachite green

4.4.4.3 Effect of Catalyst dosage

Experiments with 5–50 mg of Fe₃O₄ nanocomposite showed that adsorption efficiency increased with catalyst dosage. The removal rate rose

from 50% at 5 mg to 61% at 20–30 mg, reaching nearly 100% at 50 mg. This indicated that higher catalyst amounts provided more active sites, enhancing MG adsorption.

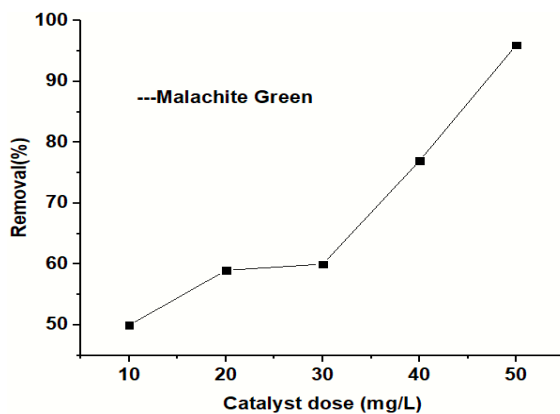


Fig. 4.13: Effect of catalyst dose on the removal of malachite green

4.4.4.4 Effect of Temperature on removal rate.

The adsorption rate decreased with increasing temperature (20–50°C), suggesting that MG adsorption was an exothermic process. At lower dye concentrations,

temperature had little effect, but at higher concentrations, increased temperature reduced adsorption efficiency (Arora *et al.*, 2022).

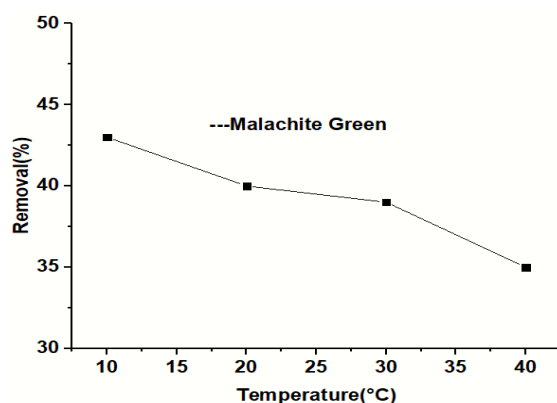


Fig. 4.14: Effect of temperature on removal of malachite green

4.5 Catalyst Recovery and Reusability

The study on catalyst recovery and reusability highlighted the importance of multi-cycle utilization for cost-effective and scalable treatment systems. The adsorbent was regenerated using ethanol and acetone after being washed with deionized water. The reusability tests showed a slight decline in adsorption efficiency (8–15%) with each cycle due to the saturation of adsorption sites by dye molecules. Despite this, the Fe₃O₄ nanocomposite maintained good adsorption performance for methyl orange (MO) and malachite green (MG) dyes, proving its effectiveness for multiple reuse cycles.

5. CONCLUSION

The present research objective was attained by synthesizing Fe₃O₄ based nanocomposite and their characterization. For this purpose, chemical co-precipitation method was used to produce desired nanocomposite as this method preferred due to its cost effective and environmental impact. UV-VIS spectroscopy confirms the synthesis of desired nanocomposites. SEM, XRD and FT-IR techniques were used for characterization of prepared sample. The maximum adsorption process of dyes was obtained by optimizing using contact time, adsorbent dosage, pH, and dye concentration. Therefore, the synthetic Fe₃O₄ based nanocomposites is an excellent adsorbent material for removal of toxic/recalcitrant dyes from Wastewater. This finding suggests that modifying moderate amount of Fe₃O₄ based nanocomposites is a feasible way of improving its adsorption ability for methyl orange and malachite green dyes. Therefore, synthetic Fe₃O₄ based nanocomposite is an excellent adsorbent material for removal of toxic dyes from wastewater.

REFERENCES

- Algar, W. R., Albrecht, T., Faulds, K., & Zhu, J.-J. (2022). Analytical nanoscience. *Analyst*, 147(5), 765-766.
- Amoli-Diva, M., Anvari, A., & Sadighi-Bonabi, R. (2019). Synthesis of magneto-plasmonic Au-Ag NPs-decorated TiO₂-modified Fe₃O₄ nanocomposite with enhanced laser/solar-driven photocatalytic activity for degradation of dye pollutant in textile wastewater. *Ceramics International*, 45(14), 17837-17846.
- Arora, B., Sharma, S., Dutta, S., Sharma, A., Yadav, S., Rana, P., Mehta, S., & Sharma, R. (2022). Design and Fabrication of a Retrievable Magnetic Halloysite Nanotubes Supported Nickel Catalyst for the Efficient Degradation of Methylviolet 6B and Acid Orange 7. *ChemistrySelect*, 7(47), e202202751.
- Bassyouni, D., Mohamed, M., El-Ashtoukhy, E.-S., Abd El-Latif, M., Zaatout, A., & Hamad, H. (2019). Fabrication and characterization of electrospun Fe₃O₄/o-MWCNTs/polyamide 6 hybrid nanofibrous membrane composite as an efficient and recoverable adsorbent for removal of Pb (II). *Microchemical Journal*, 149, 103998.
- Brazell, L. (2012). *Nanotechnology law: best practices*. Kluwer Law International BV.
- Cai, H., Feng, C., Xiao, H., & Cheng, B. (2022). Synthesis of Fe₃O₄/rGO@ PANI with three-dimensional flower-like nanostructure and microwave absorption properties. *Journal of Alloys and Compounds*, 893, 162227.
- Chen, J., Wang, F., Huang, K., Liu, Y., & Liu, S. (2009). Preparation of Fe₃O₄ nanoparticles with adjustable morphology. *Journal of Alloys and Compounds*, 475(1-2), 898-902.
- Chen, T., Geng, Y., Wan, H., Xu, Y., Zhou, Y., Kong, X., Wang, J., Qi, Y., Yao, B., & Gao, Z. (2021). Facile preparation of Fe₃O₄/Ag/RGO reusable ternary nanocomposite and its versatile application as catalyst and antibacterial agent. *Journal of Alloys and Compounds*, 876, 160153.
- Cuana, R., Panre, A. M., Istiqomah, N. I., Tumbelaka, R. M., Wicaksono, S. T., & Suharyadi,

- E. (2022). Green synthesis of Fe₃O₄/chitosan nanoparticles utilizing Moringa Oleifera extracts and their surface plasmon resonance properties. *ECS Journal of Solid State Science and Technology*, 11(8), 083015.
- Dudchenko, N., Pawar, S., Perelshtein, I., & Fixler, D. (2022). Magnetite nanoparticles: Synthesis and applications in optics and nanophotonics. *Materials*, 15(7), 2601.
 - Elazab Dr, H. A. (2019). Optimization of the catalytic performance of Pd/Fe₃O₄ nanoparticles prepared via microwave-assisted synthesis for pharmaceutical and catalysis applications.
 - Eskandarinezhad, S., Khosravi, R., Amarzadeh, M., Mondal, P., & Magalhães Filho, F. J. C. (2021). Application of different Nanocatalysts in industrial effluent treatment: A review. *Journal of Composites and Compounds*, 3(6), 43-56.
 - Garcia, C. V., Shin, G. H., & Kim, J. T. (2018). Metal oxide-based nanocomposites in food packaging: Applications, migration, and regulations. *Trends in food science & technology*, 82, 21-31.
 - Kirtane, A. R., Verma, M., Karandikar, P., Furin, J., Langer, R., & Traverso, G. (2021). Nanotechnology approaches for global infectious diseases. *Nature Nanotechnology*, 16(4), 369-384.
 - Koo, K. N., Ismail, A. F., Othman, M. H. D., Bidin, N., & Rahman, M. A. (2019). Preparation and characterization of superparamagnetic magnetite (Fe₃O₄) nanoparticles: A short review. *Malaysian Journal of Fundamental and Applied Sciences*, 15(1), 23-31.
 - Kumar, A., & Gangawane, K. M. (2022). Synthesis and effect on the surface morphology & magnetic properties of ferrimagnetic nanoparticles by different wet chemical synthesis methods. *Powder Technology*, 410, 117867.
 - Magdalane, C. M., Kaviyarasu, K., Vijaya, J. J., Jayakumar, C., Maaza, M., & Jeyaraj, B. (2017). Photocatalytic degradation effect of malachite green and catalytic hydrogenation by UV-illuminated CeO₂/CdO multilayered nanoplatelet arrays: investigation of antifungal and antimicrobial activities. *Journal of Photochemistry and Photobiology B: Biology*, 169, 110-123.
 - Mahmoodabadi, A. N., Kompany, A., & Mashreghi, M. (2018). Characterization, antibacterial and cytotoxicity studies of graphene-Fe₃O₄ nanocomposites and Fe₃O₄ nanoparticles synthesized by a facile solvothermal method. *Materials Chemistry and Physics*, 213, 285-294.
 - Miharayan, A., Ferraz, N., & Strømme, M. (2012). Current status and future prospects of nanotechnology in cosmetics. *Progress in materials science*, 57(5), 875-910.
 - Mishra, P., Patnaik, S., & Parida, K. (2019). An overview of recent progress on noble metal modified magnetic Fe₃O₄ for photocatalytic pollutant degradation and H₂ evolution. *Catalysis Science & Technology*, 9(4), 916-941.
 - Namvar, F., Rahman, H. S., Mohamad, R., Baharara, J., Mahdavi, M., Amini, E., Chartrand, M. S., & Yeap, S. K. (2014). Cytotoxic effect of magnetic iron oxide nanoparticles synthesized via seaweed aqueous extract. *International Journal of Nanomedicine*, 2479-2488.
 - Norfolk, L. (2021). *A Bioinspired Approach to the Synthesis and Scale-up of Bespoke Magnetite Nanoparticles* University of Sheffield].
 - Novoselova, L. Y. (2021). Nanoscale magnetite: New synthesis approach, structure and properties. *Applied Surface Science*, 539, 148275.
 - Parhi, R. (2022). Recent advances in microneedle designs and their applications in drug and cosmeceutical delivery. *Journal of Drug Delivery Science and Technology*, 75, 103639.
 - Rasoulzadeh, H., Mohseni-Bandpei, A., Hosseini, M., & Safari, M. (2019). Mechanistic investigation of ciprofloxacin recovery by magnetite-imprinted chitosan nanocomposite: isotherm, kinetic, thermodynamic and reusability studies. *International journal of biological macromolecules*, 133, 712-721.
 - Rostami, Z., Rouhanizadeh, M., Nami, N., & Zareyee, D. (2018). Fe₃O₄ magnetic nanoparticles (MNPs) as an effective catalyst for synthesis of indole derivatives. *Nanochemistry Research*, 3(2), 142-148.
 - Sarojini, G., Kannan, P., Rajamohan, N., & Rajasimman, M. (2023). Bio-fabrication of porous magnetic Chitosan/Fe₃O₄ nanocomposite using *Azolla pinnata* for removal of chromium—Parametric effects, surface characterization and kinetics. *Environmental Research*, 218, 114822.
 - Shekofteh-Gohari, M., & Habibi-Yangjeh, A. (2016). Novel magnetically separable ZnO/AgBr/Fe₃O₄/Ag₃VO₄ nanocomposites with tandem n-n heterojunctions as highly efficient visible-light-driven photocatalysts.
 - Sinitsyna, V. V., & Vetcher, A. A. (2022). Nucleic acid aptamers in nanotechnology. *Biomedicines*, 10(5), 1079.
 - Taha, A. B., Essa, M. S., & Chiad, B. T. (2022). Spectroscopic study of iron oxide nanoparticles synthesized via hydrothermal method. *Chem. Methodol*, 6(12), 977-984.
 - Thu, T. V., Ko, P. J., Nguyen, T. V., Vinh, N. T., Khai, D. M., & Lu, L. T. (2017). Green synthesis of reduced graphene oxide/Fe₃O₄/Ag ternary nanohybrid and its application as magnetically recoverable catalyst in the reduction of 4-nitrophenol. *Applied Organometallic Chemistry*, 31(11), e3781.
 - Wang, L., & Yan, Y. (2021). A Review of pH-Responsive Organic-Inorganic Hybrid Nanoparticles for RNAi-Based Therapeutics. *Macromolecular Bioscience*, 21(9), 2100183.

- Wang, R., Cai, Y., Su, Z., Ma, X., & Wu, W. (2022). High positively charged Fe₃O₄ nanocomposites for efficient and recyclable demulsification of hexadecane-water micro-emulsion. *Chemosphere*, 291, 133050.
- Xu, P., Han, X., Zhang, B., Du, Y., & Wang, H.-L. (2014). Multifunctional polymer-metal nanocomposites via direct chemical reduction by conjugated polymers. *Chemical Society Reviews*, 43(5), 1349-1360.
- Yadav, B. S., & Dasgupta, S. (2022). Effect of time, pH, and temperature on kinetics for adsorption of methyl orange dye into the modified nitrate intercalated MgAl LDH adsorbent. *Inorganic Chemistry Communications*, 137, 109203.
- Yilmaz, M., Mengelizadeh, N., khodadadi Saloot, M., & Balarak, D. (2022). Facile synthesis of Fe₃O₄/ZnO/GO photocatalysts for decolorization of acid blue 113 under solar, visible and UV lights. *Materials Science in Semiconductor Processing*, 144, 106593.
- Zhu, X., Zhang, L., Zou, G., Chen, Q., Guo, Y., Liang, S., Hu, L., North, M., & Xie, H. (2021). Carboxylcellulose hydrogel confined-Fe₃O₄ nanoparticles catalyst for Fenton-like degradation of Rhodamine B. *International journal of biological macromolecules*, 180, 792-803.